

## Synchronized Chaos in Geophysical Fluid Dynamics

Gregory S. Duane\* and Joseph J. Tribbia

National Center for Atmospheric Research, P.O. Box 3000, Boulder, Colorado 80307

(Received 5 September 2000)

Fluid flow fields in a pair of quasi-two-dimensional channel models, each of which vacillates chaotically between distinct flow regimes, synchronize if only the small-scale eddy components of the two flows are coupled. The synchronization behavior also governs the relationship between different sectors of the same continuous channel. Where there is no natural boundary to define the sectors, but the sectors are separately forced, the channel can be represented as two coextensive, coupled channel models with different forcing terms. Generalized synchronization of these two systems implies a relationship between the Atlantic and Pacific sectors of the Earth's climate system.

DOI: 10.1103/PhysRevLett.86.4298

PACS numbers: 47.52.+j, 05.45.Xt, 92.70.Gt

It has been established in the past decade that loosely coupled chaotic oscillators will fall into stably synchronized motion along their strange attractors, irrespective of initial conditions, in a wide variety of scenarios [1]. However, in contrast to the ubiquitous synchronization of oscillators with limit cycle attractors in nature, the widespread occurrence of synchronized chaotic oscillators in naturally occurring systems has not been demonstrated. Rather, the phenomenon of synchronized chaos has been explored primarily in low-order or man-made systems, primarily for applications to secure communications. More recently, chaos synchronization was demonstrated in spatially extended systems [2], and a vestige of synchronization in low-order systems with time-lagged coupling was proposed to explain "teleconnection patterns" linking weather phenomena in widely separated regions of the Earth's atmosphere [3,4]. This previous study relied on a severe truncation of the partial differential equations of geophysical fluid dynamics to generate a low-order system, which was then coupled, using a wave-dynamical ansatz, to another such system representing the opposite hemisphere. The behavior of such low-order truncations of fluid-dynamical systems varies qualitatively with order of truncation. In this Letter we present a more general synchronization scenario: A pair of fully resolved quasi-2D fluid models will synchronize when only the small-scale/high-frequency components of the flow are coupled. Such synchronous coupling is key to explaining the relationship between different sectors of the same continuous channel in a model of the large-scale atmospheric flow. In a system whose parts are strongly coupled, with no natural boundary between them, the definition of subsystems on which to base a study of synchronization may not be obvious. Here, we use the fact that the two sectors of the channel have distinct forcing mechanisms, in the realistic case of Atlantic/Pacific coupling, to unfold the system into two coupled models of the entire channel, each model with different forcing terms, in order to demonstrate the implications of eddy-induced synchronization for the intersectorial correspondence between states. As with the related phenomenon of controlled

chaos, which was recently shown to apply to a model of the El Niño cycle [5], synchronized chaos is thus shown to be relevant to the behavior of the Earth's atmosphere, and to many other naturally occurring fluid systems.

We consider a model of fluid flow in a two-layer channel given by the following equation for the time derivative of potential vorticity  $q$ :

$$\frac{Dq_i}{Dt} \equiv \frac{\partial q_i}{\partial t} + J(\psi_i, q_i) = F_i + D_i, \quad (1)$$

where the layer  $i = 1, 2$ ,  $\psi$  is the stream function, and the Jacobian  $J(\psi, \cdot) = \frac{\partial \psi}{\partial x} \frac{\partial \cdot}{\partial y} - \frac{\partial \psi}{\partial y} \frac{\partial \cdot}{\partial x}$  gives the advective contribution to the comoving ("Lagrangian") derivative  $D/Dt$ . Equation (1) states that potential vorticity is conserved on a moving parcel (generalizing the conservation of angular momentum to a continuous medium in a nonuniformly rotating frame and accounting for the possibility of vortex stretching in each layer), except for forcing  $F_i$  and dissipation  $D_i$ . The discretized potential vorticity is

$$q_i = f_0 + \beta y + \nabla^2 \psi_i + R_i^{-2} (\psi_1 - \psi_2) (-1)^i, \quad (2)$$

where  $f(x, y)$  is the vorticity due to the Earth's rotation at each point  $(x, y)$ ,  $f_0$  is the average  $f$  in the channel,  $\beta$  is the constant  $df/dy$ , and  $R_i$  is the Rossby radius of deformation in each layer (defined in Ref. [6]). Periodic boundary conditions are imposed in the longitudinal  $x$  dimension. The form of the dissipation terms  $D_i$ , parameter values, and other details are based on Ref. [7], except that the width of the channel is half the length and a second channel (not shown in the figures), with flow in the opposite direction, is used to join the upper and lower latitudinal boundaries, in place of the free slip boundary conditions used in [7]. This *quasigeostrophic* model provides a good approximation to the nearly two-dimensional atmospheric flow in a rotating frame [6]. If the forcing is chosen to be a relaxation term  $F_i = \mu_0(q_i^* - q_i)$ , the flow will tend to a jetlike form near the beginning of the channel, for  $q_i^*$  defined by the forcing stream function  $\psi_i^*$  shown in Fig. 1a, via (2). For appropriately chosen dissipation  $D_i$ , the model will then vacillate chaotically between two relatively stable flow regimes that naturally divide state space, illustrated

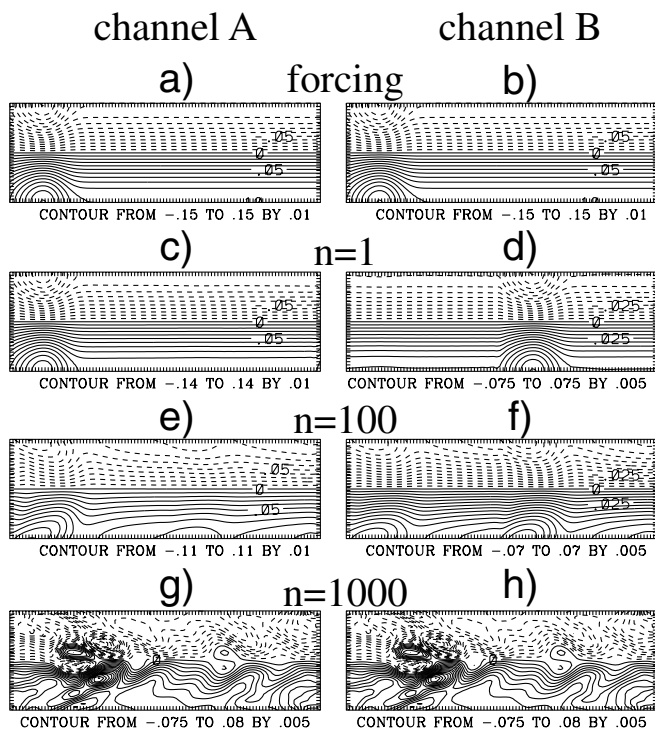


FIG. 1. Stream function (in units of  $1.48 \times 10^9 \text{ m}^2 \text{ s}^{-1}$ ) describing the forcing  $\psi^*$  (a),(b), and the evolving flow  $\psi$  (c)–(h), in the parallel channel model with dissipative coupling of the eddies [given by (1), (3), and (4), in conjunction with Ref. [7]], for the indicated numbers  $n$  of time steps in a numerical integration. An average stream function for the two vertical layers  $i = 1, 2$  is shown. One time step is  $\approx 0.4$  h. The relaxation time  $1/\mu_0$  defining the coupling strength is on the order of one time step. Synchronization occurs by the last time shown (g),(h), despite differing initial conditions.

for instance by the flows in Figs. 1e and 1g, which are usually referred to as “zonal” and “blocked,” respectively [7]. The division into these state space regimes is also of practical interest because blocked flow interrupts the normal progression of weather patterns from west to east and results in extreme weather conditions.

We now couple two models of the form (1), imagining a physically unrealizable configuration in which each point in a given layer of one model is coupled to the corresponding point in the corresponding layer of the other model. The coupling is given by a modified forcing term:

$$\begin{aligned} F_{\mathbf{k}}^A &= \mu_{\mathbf{k}}^c [q_{\mathbf{k}}^B - q_{\mathbf{k}}^A] + (\mu_0 - \mu_{\mathbf{k}}^c) [q_{\mathbf{k}}^* - q_{\mathbf{k}}^A], \\ F_{\mathbf{k}}^B &= \mu_{\mathbf{k}}^c [q_{\mathbf{k}}^A - q_{\mathbf{k}}^B] + (\mu_0 - \mu_{\mathbf{k}}^c) [q_{\mathbf{k}}^* - q_{\mathbf{k}}^B], \end{aligned} \quad (3)$$

where the flow has been decomposed spectrally and the subscript  $\mathbf{k}$  on each quantity indicates the wave number  $\mathbf{k}$  spectral component. The superscripts  $A$  and  $B$  designate the two separate channel models, each of which has two layers. The layer index  $i$  has been suppressed in (3) and will be suppressed henceforth. If the coupling coefficient  $\mu_{\mathbf{k}}^c$  is allowed to vary with the wave number, then we can arrange to couple the small-scale/high-frequency compo-

nents (the “eddies”) while leaving the large-scale modes uncoupled, by setting

$$\begin{aligned} \mu_{\mathbf{k}}^c &= 0, & \text{if } |k_x| \leq k_{x0} \text{ and } |k_y| \leq k_{y0}, \\ \mu_{\mathbf{k}}^c &= \mu_0 [1 - (k_0/|\mathbf{k}|)^4] & \text{otherwise,} \end{aligned} \quad (4)$$

defining a slightly smoothed step function. Following Ref. [7], we set the wave number cutoffs  $k_{x0} = 3$  and  $k_{y0} = 2$  (in units of waves per channel length or width, respectively) to distinguish between eddies and the large-scale flow. It is found that with the coupling so defined, the flows in the two channels synchronize completely, regardless of initial conditions, as illustrated in Fig. 1. Synchronization does not occur in the opposite coupling scenario where only the large-scale modes are coupled. Of course, synchronization does occur if all modes are coupled. The phenomenon is patently independent of the resolution of the model, and occurs even when the geophysical constants  $\beta$  and  $f$  vanish.

To show the relevance of synchronization in the parallel channel model to a physical situation, we consider the following modifications: First, we place the jets in the two channels in different positions, skewed in the  $x$  dimension, so that  $q^{A*} \neq q^{B*}$ , as shown in Figs. 2a and 2b. Second, we use the nonstandard coupling:

$$\frac{Dq^A}{Dt} + cJ(\psi^A, q^B - q^A) = F^A + D, \quad (5a)$$

$$\frac{Dq^B}{Dt} + cJ(\psi^B, q^A - q^B) = F^B + D, \quad (5b)$$

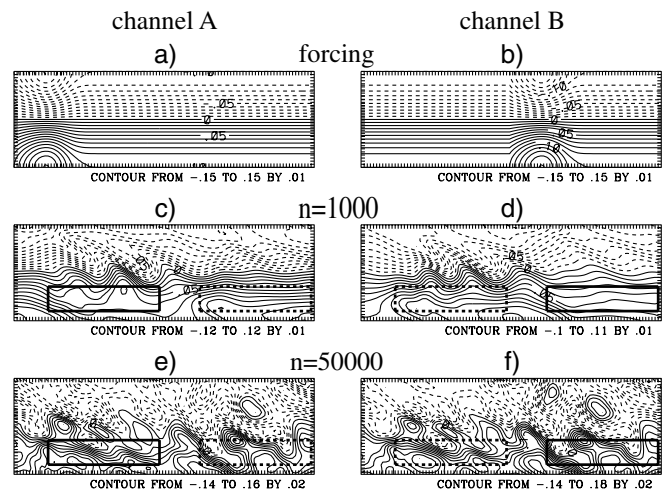


FIG. 2. Stream function describing the forcing and evolution of a coupled parallel channel model as in Fig. 1, but with longitudinally skewed forcing jets  $\psi^{A*} \neq \psi^{B*}$  (a),(b) and advective coupling [Eqs. (5) and (6)], with  $c = 1/2$ . Near-identical synchronization occurs by the last time step shown (e),(f). The solid-line boxes designate the regions in the two channels used to label a given flow as “blocked” or “zonal.” Blocking activity in the dashed-line box in channel A, which is nearly the same as in the solid-line box in channel B after synchronization, anticorrelates with blocking in the solid-line box in channel A (similarly for the dashed-line box in channel B).

that is, we introduce the coupling in the advection terms instead of in the forcing terms. The forcing  $F^{A,B}$  is given by the second term in (3), i.e.,

$$F_{\mathbf{k}}^{A,B} = (\mu_0 - \mu_{\mathbf{k}}^c)[q_{\mathbf{k}}^{(A,B)*} - q_{\mathbf{k}}^{A,B}], \quad (6)$$

which dynamically constrains the large-scale components, but not the eddies. The synchronization of two chaotic systems is commonly robust against variations in the form of the coupling, and indeed, the coupled channels are found to synchronize (albeit less stably) with the advective coupling (5), as seen in Fig. 2. While the systems cannot exhibit identical synchronization as before, since  $q^{A*} \neq q^{B*}$ ,  $F^A \neq F^B$ , the correspondence that defines the generalized synchronization [8] between the flow patterns is very close to the identity, as seen in the figure. We next note that the average  $\hat{q} = (q^A + q^B)/2$  of the solutions of (5a) and (5b), for strong coupling  $c = 1/2$ , is the solution of a model with the average forcing, which folds the two channels together:

$$\begin{aligned} \left(\frac{D\hat{q}}{Dt}\right)_{\mathbf{k}} &= 1/2(F_{\mathbf{k}}^A + F_{\mathbf{k}}^B) + \hat{D}_{\mathbf{k}} \\ &= (\mu_0 - \mu_{\mathbf{k}}^c)[1/2(q_{\mathbf{k}}^{A*} + q_{\mathbf{k}}^{B*}) - \hat{q}_{\mathbf{k}}] + \hat{D}_{\mathbf{k}}, \end{aligned} \quad (7)$$

since the advective coupling terms in (5) combine to give the proper nonlinear advective term in (7). The potential vorticity  $\hat{q}$  is thus the solution for the single channel model shown in Fig. 3, which has two sectors, each forced by a separate jet. [Synchronization also occurs when only the small-scale components are included in the advective coupling term in (5)]. Because of the synchronization, we have  $\hat{q} \approx q^A \approx q^B$ , so the solutions of the unphysical parallel channel model, for  $c = 1/2$ , are also approximate solutions of the physical two-sector model. For  $0 < c < 1/2$ , the two single-sector models are partially coupled.

The two sectors of the channel can be taken to represent the Atlantic and Pacific sectors of the Northern Hemisphere midlatitude region, since the simpler channel model given by (1) was intended to represent either one of these sectors, considered in isolation. There is an upper tropospheric jet over each ocean that drives blocked/zonal flow vacillation in the corresponding sector. The periodic

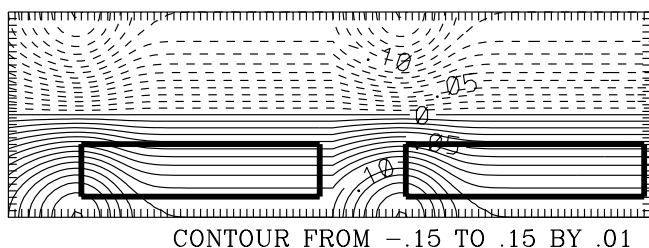


FIG. 3. The forcing stream function  $\hat{\psi}^*$  for the two-sector model (7), with one jet in each sector. At any given time, the flow in each sector is labeled as “blocked” or “zonal,” depending on whether the minimum, taken over all longitudes  $x$  in the box in that sector, of the difference in stream function  $\psi$  latitudinally across the box, is less than or greater than 0.01 (in the units of Fig. 1), respectively.

boundary conditions imposed on the single-sector models are taken to represent the actual topology of a midlatitude band on the Earth’s surface, but with the opposite sector assumed to be passive. The two channels in the system (5) with no coupling ( $c = 0$ ) would crudely represent the Atlantic sector with a jetless Pacific, and a Pacific sector with a jetless Atlantic, respectively. As the coupling between the channels is increased, the dynamics of each channel changes so as to incorporate an approximate, “virtual” counterpart of the dynamics of the sector that is forced in the other channel. For some coupling value  $c < 1/2$ , the channels synchronize. The type of chaos synchronization exhibited here, in which the dynamics of the two systems change when they are coupled, is generally important for strong coupling.

The relationship between the two sectors is given by the correspondence that defines the synchronization manifold. Although this correspondence is near to the identity in the representation suggested by Fig. 2, corresponding states in the two channels are *described* very differently, giving rise to an instance of *generalized synchronization* in the manner of the original formulation of that concept [8]. While the state of channel A is characterized as blocked or zonal depending on the flow in the first half of the channel, in the area denoted by the solid box in Fig. 2, just downstream of the channel’s driving jet, the state of channel B is similarly characterized depending on the flow in the second half of the channel. It turns out that blocking activity is weakly anticorrelated in the two halves of either channel, whether

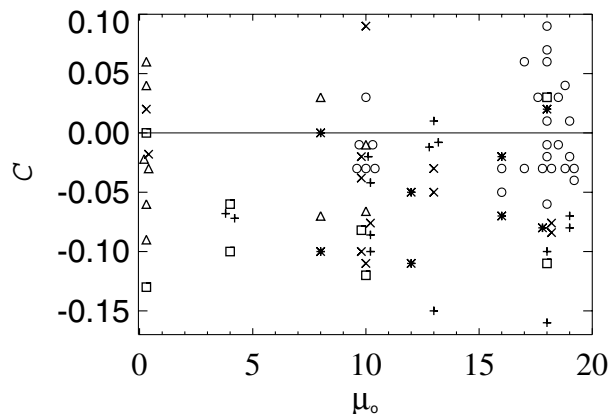


FIG. 4. Correlation between binarized (blocked vs zonal) states of the two sectors of the model illustrated in Fig. 3, with the binarization as defined in the caption thereto, in numerical integrations of (7) over  $4 \times 10^5$  time steps with arbitrarily chosen initial conditions. The horizontal axis is the forcing strength  $\mu_0$  (in units of  $7.3 \times 10^{-5} \text{ s}^{-1}$ ).  $\times$ 's denote correlations for the two-sector model as previously defined, squares are for a variant with one sector two-thirds as long as the other, triangles are for one sector one-half as long as the other,  $*$ 's are for shortened jets in both sectors,  $+$ 's are for lengthened jets in both sectors, and circles are for a variant in which the latitudinal positions of the two jets are skewed arbitrarily by shifts ranging from a channel half-width to a channel width. Significant anticorrelation is found in all model variants, for  $\mu_0$  not too small, except in the case of latitudinally skewed jets.

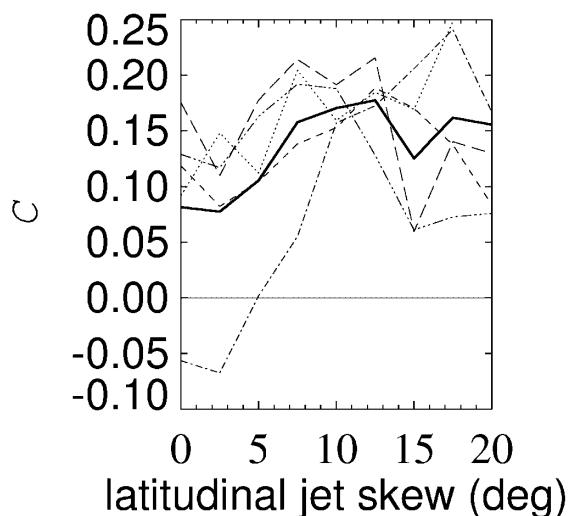


FIG. 5. Correlation between blocking activity in the Atlantic ( $100^{\circ}$  W– $100^{\circ}$  E) and Pacific ( $100^{\circ}$  E– $100^{\circ}$  W) sectors, in observed meteorological data, on days of given latitudinal skew between Atlantic and Pacific jet positions. The data and blocking definitions are as in Ref. [3], except Northern Hemisphere winters for the 40 yr period 1958–1998 are considered. Daily jet position is defined as the position of the maximum eastward component of wind, in the same observational data set, at an altitude corresponding to a pressure level of 300 mb, at non-blocked longitudes. Correlations are shown for the full 40-yr period (solid line) and for five 8-yr segments (five broken lines). The partitioning demonstrates that the increase in correlation as the skew increases from  $0^{\circ}$  to  $10^{\circ}$  is statistically significant.

or not the channels are synchronously coupled. (For  $c = 0$ , anticorrelation is suggested by the detailed study of the single-sector model by Vautard and Legras, who showed that the eddies induced by a blocked flow pattern tend to maintain that pattern, but that the eddies weakly inhibit blocking at other locations [9].) Synchronization therefore implies anticorrelation between blocking in the two sectors. That is to say, the correspondence defining generalized synchronization, described in natural variables, is very far from the identity and implies anticorrelation in a natural binarization of the state spaces [10].

Since blocking is defined nonlinearly in terms of the flow field, anticorrelation in the average field  $\hat{q}$  does not follow generally from anticorrelation within the two parallel channels separately, but does follow in the synchronous case where  $\hat{q} \approx q^A \approx q^B$ . Weak anticorrelation is indeed found in the two-sector model, as seen in Fig. 4 for several variants of the model. The effect is induced by exchange of eddies. If a  $\mathbf{k}$ -independent forcing is used instead of (6), as in the original single-sector model, so that the eddies are not free to mediate a sufficiently strong coupling, then both the synchronization in the parallel channel model and the anticorrelation in the two-sector model are found to disappear.

The prediction that the exchange of eddies between the Atlantic and Pacific sectors causes anticorrelation of blocking activity cannot be directly compared with observations because the treatment of the large-scale flow in the model

is unrealistic. In reality, the velocities and other characteristics of the jets vary. When the mass transport is high, blocking is less likely, so that coupling between the large-scale components results in a *correlating* effect that competes with anticorrelation due to eddy exchange. A full analysis of this competition will be given in a longer paper. Here, we note a way in which the masked anticorrelation might still be detected in meteorological observations. It is found in the model that the anticorrelation effect, while rather robust against most changes in flow configuration, tends to disappear when the jets are skewed latitudinally (i.e., in the  $y$  direction), as illustrated by correlation values (circles) plotted in Fig. 4. This finding agrees with the observation in Fig. 5 that correlation in blocking activity is enhanced on days when the upper tropospheric jets over the Atlantic and Pacific are skewed in a latitudinal position, by shifts up to  $10^{\circ}$ .

As to the generality of the results presented here: It cannot be expected that the eddy-induced synchronization phenomenon will carry over to full three-dimensional fluid flow, because of the well-known difference in the direction of energy cascade between 2D and 3D flows. But in the many situations where a 2D approximation applies, the fact that eddies exchanged between parallel channels cause flows to synchronize will be of consequence.

One of us (G.S.D.) thanks Peter Webster for encouraging his early ideas about synchronized chaos in meteorology. The National Center for Atmospheric Research is sponsored by the National Science Foundation.

---

\*Email address: gduane@ucar.edu

- [1] H. Fujisaka and T. Yamada, *Prog. Theor. Phys.* **69**, 32 (1983); V.S. Afraimovich, N.N. Verichev, and M.I. Rabinovich, *Radiophys. Quantum Electron.* **29**, 795 (1986); L.M. Pecora and T.L. Carroll, *Phys. Rev. Lett.* **64**, 821 (1990); L.M. Pecora, T.L. Carroll, G.A. Johnson, and D.J. Mar, *Chaos* **7**, 520 (1997).
- [2] L. Kocarev, Z. Tasev, and U. Parlitz, *Phys. Rev. Lett.* **79**, 51 (1997).
- [3] G.S. Duane, *Phys. Rev. E* **56**, 6475 (1997).
- [4] G.S. Duane, P.J. Webster, and J.B. Weiss, *J. Atmos. Sci.* **56**, 4183 (1999).
- [5] E. Tziperman, H. Scher, S.E. Zebiak, and M.A. Cane, *Phys. Rev. Lett.* **79**, 1034 (1997).
- [6] J. Pedlosky, *Geophysical Fluid Dynamics* (Springer-Verlag, Berlin, 1987).
- [7] R. Vautard, B. Legras, and M. Déqué, *J. Atmos. Sci.* **45**, 2811 (1988); R. Vautard and B. Legras, *J. Atmos. Sci.* **45**, 2845 (1988).
- [8] N.F. Rulkov *et al.*, *Phys. Rev. E* **51**, 980 (1995).
- [9] See Ref. [7], p. 2855, Figs. 6g,h.
- [10] It is noted that a similar anticorrelation was found in Ref. [4] for weakly coupled models of the Northern and Southern Hemispheres, in the analogous situation where the forcing mechanisms, based on topographic features that played the role of the jets used here, were skewed longitudinally.